



This is a repository copy of *Impact ionization coefficients and excess noise in Al<sub>0.55</sub>Ga<sub>0.45</sub>As<sub>0.56</sub>Sb<sub>0.44</sub> lattice matched to InP.*

White Rose Research Online URL for this paper:  
<https://eprints.whiterose.ac.uk/215583/>

Version: Published Version

---

**Article:**

Jin, X. [orcid.org/0000-0002-7205-3318](https://orcid.org/0000-0002-7205-3318), Lewis, H.I.J. [orcid.org/0000-0003-4698-4300](https://orcid.org/0000-0003-4698-4300), Yi, X. [orcid.org/0000-0003-0177-2398](https://orcid.org/0000-0003-0177-2398) et al. (5 more authors) (2024) Impact ionization coefficients and excess noise in Al<sub>0.55</sub>Ga<sub>0.45</sub>As<sub>0.56</sub>Sb<sub>0.44</sub> lattice matched to InP. *Applied Physics Letters*, 124 (25). 251104. ISSN 0003-6951

<https://doi.org/10.1063/5.0214617>

---

**Reuse**

This article is distributed under the terms of the Creative Commons Attribution (CC BY) licence. This licence allows you to distribute, remix, tweak, and build upon the work, even commercially, as long as you credit the authors for the original work. More information and the full terms of the licence here:  
<https://creativecommons.org/licenses/>

**Takedown**

If you consider content in White Rose Research Online to be in breach of UK law, please notify us by emailing [eprints@whiterose.ac.uk](mailto:eprints@whiterose.ac.uk) including the URL of the record and the reason for the withdrawal request.



[eprints@whiterose.ac.uk](mailto:eprints@whiterose.ac.uk)  
<https://eprints.whiterose.ac.uk/>

RESEARCH ARTICLE | JUNE 18 2024

# Impact ionization coefficients and excess noise in $\text{Al}_{0.55}\text{Ga}_{0.45}\text{As}_{0.56}\text{Sb}_{0.44}$ lattice matched to InP

Xiao Jin ; Harry I. J. Lewis ; Xin Yi ; Shiyu Xie; Baolai Liang  ; Diana L. Huffaker; Chee Hing Tan ; John P. R. David  

 Check for updates

*Appl. Phys. Lett.* 124, 251104 (2024)

<https://doi.org/10.1063/5.0214617>



View Online



Export Citation

06 August 2024 08:12:51



Nanotechnology & Materials Science



Optics & Photonics



Impedance Analysis



Scanning Probe Microscopy



Sensors



Failure Analysis & Semiconductors



**Unlock the Full Spectrum.**  
From DC to 8.5 GHz.

Your Application. Measured.

[Find out more](#)



# Impact ionization coefficients and excess noise in $\text{Al}_{0.55}\text{Ga}_{0.45}\text{As}_{0.56}\text{Sb}_{0.44}$ lattice matched to InP

Cite as: Appl. Phys. Lett. **124**, 251104 (2024); doi: [10.1063/5.0214617](https://doi.org/10.1063/5.0214617)

Submitted: 18 April 2024 · Accepted: 9 June 2024 ·

Published Online: 18 June 2024



View Online



Export Citation



CrossMark

Xiao Jin,<sup>1</sup> Harry I. J. Lewis,<sup>1,a)</sup> Xin Yi,<sup>2</sup> Shiyu Xie,<sup>3,b)</sup> Baolai Liang,<sup>4,c)</sup> Diana L. Huffaker,<sup>3,4,d)</sup> Chee Hing Tan,<sup>1</sup> and John P. R. David<sup>1,c)</sup>

## AFFILIATIONS

<sup>1</sup>Department of Electronic and Electrical Engineering, University of Sheffield, Sheffield S1 3JD, United Kingdom

<sup>2</sup>Institute of Photonics and Quantum Science, School of Engineering and Physics Sciences, Heriot-Watt University, David Brewster Building, Edinburgh EH14 4AS, United Kingdom

<sup>3</sup>School of Physics and Astronomy, Cardiff University, Queen's Building, The Parade, Cardiff CF24 3AA, United Kingdom

<sup>4</sup>California NanoSystems Institute, University of California, Los Angeles, California 90095, USA

<sup>a)</sup>Present address: TRIUMF, 4004 Westbrook Mall, Vancouver, British Columbia V6T 2A3, Canada.

<sup>b)</sup>Present address: Microsemi Ltd, Shanghai 200001, China.

<sup>c)</sup>Authors to whom correspondence should be addressed: [bliang@cnsi.ucla.edu](mailto:bliang@cnsi.ucla.edu) and [j.p.david@sheffield.ac.uk](mailto:j.p.david@sheffield.ac.uk)

<sup>d)</sup>Present address: Electrical Engineering Department, The University of Texas at Arlington, Texas 76019, USA.

## ABSTRACT

The avalanche multiplication and noise characteristics of  $\text{Al}_{0.55}\text{Ga}_{0.45}\text{As}_{0.56}\text{Sb}_{0.44}$   $p-i-n$  and  $n-i-p$  structures grown lattice matched on InP have been investigated. From measurements undertaken using 530 nm illumination on several devices, the electron ( $\alpha$ ) and hole ( $\beta$ ) impact ionization coefficients have been determined. While  $\alpha$  only shows a relatively small increase compared to the higher Al composition alloys of  $\text{Al}_x\text{Ga}_{1-x}\text{AsSb}$ ,  $\beta$  is found to increase significantly. Although the  $\beta/\alpha$  ratio is increased to  $\sim 0.125$ – $0.2$ , higher than the  $\sim 0.003$ – $0.02$  seen in the higher-Al alloys, a relatively low excess noise factor of 2.2 was measured in the  $p-i-n$  with electron-initiated multiplication of 20. This noise performance is significantly lower than that predicted using a local-field model and comparable to some commercial silicon APDs. This avalanching material with a bandgap of  $\sim 1.24$  eV will have the advantages of a smaller band discontinuity with the absorber region and should also operate at a lower voltage.

© 2024 Author(s). All article content, except where otherwise noted, is licensed under a Creative Commons Attribution (CC BY) license (<https://creativecommons.org/licenses/by/4.0/>). <https://doi.org/10.1063/5.0214617>

Avalanche photodiodes (APDs) are used in various photon-starved applications, offering enhanced sensitivity in comparison with conventional  $p-i-n$  diodes due to their internal multiplication, which is provided by the process of impact ionization. However, the stochastic nature of this process results in an excess noise factor ( $F$ ), which increases with multiplication, as described by McIntyre's local field theory,<sup>1</sup>

$$F = kM + \left(2 - \frac{1}{M}\right)(1 - k), \quad (1)$$

where “ $k$ ” represents the ratio between the hole ( $\beta$ ) and electron ( $\alpha$ ) ionization coefficients, such that  $k = \beta/\alpha$  for multiplication initiated by electrons. The ionization coefficients denote the mean distance that a carrier of a given type travels between impact ionization events and are a function of electric field. The value of  $F$  sets a limit on the maximum useful multiplication achievable by a given APD before the

overall signal to noise ratio ceases to improve further. Materials with a small  $k$  value, which practically means that one carrier type ionizes much more readily than the other, produce high-performance APDs due to their reduced excess noise factor. It is therefore important that the characterization of semiconductor materials includes an accurate knowledge of  $\alpha$  and  $\beta$ . These are related to the multiplication by

$$M(x) = \frac{\exp\left[-\int_0^x (\alpha(x') - \beta(x')) dx'\right]}{1 - \int_0^W \alpha(x') \exp\left[-\int_0^{x'} (\alpha(x'') - \beta(x'')) dx''\right] dx'}, \quad (2)$$

where  $x$  is the position of carriers within the high-field region of a device and  $W$  is the total width of the high-field region.

Silicon produces APDs with high multiplication and low excess noise due to its small  $k$ , but its ability to detect photons is limited to

wavelengths below  $\lambda = 1100$  nm. To detect wavelengths out to  $\lambda = 1650$  nm, most APDs integrate an InGaAs absorber with an InP or InAlAs multiplication region in a separate absorber, charge, and multiplication region (SACM) configuration grown lattice matched on InP substrates. Unfortunately, InP<sup>2</sup> and InAlAs<sup>3</sup> have poor excess noise, equivalent to  $k = 0.4$  and  $k = 0.2$ , respectively. Recent research into  $\text{Al}_x\text{Ga}_{1-x}\text{As}_{0.56}\text{Sb}_{0.44}$  on InP (hereafter AlGaAsSb), starting with the work by Yi *et al.*<sup>4</sup> on AlAsSb, shows that this alloy exhibits a very small  $\beta/\alpha$  ratio, yielding extremely low excess noise equivalent to a  $k$  value of 0.005 in a  $t = 1550$  nm  $p$ - $i$ - $n$  structure.<sup>5</sup> Subsequent work on  $\text{Al}_{0.85}\text{Ga}_{0.15}\text{AsSb}$  also shows a small  $\beta/\alpha$  ratio<sup>6</sup> and sub-McIntyre excess noise behavior.<sup>7</sup> A number of SACM APD structures have been demonstrated with low excess noise at  $\lambda = 1550$  nm using GaAsSb<sup>8</sup> and InGaAs<sup>9</sup> absorption regions. Most recently, work on  $\text{Al}_{0.75}\text{Ga}_{0.25}\text{AsSb}$  has shown even better excess noise characteristics of  $F = 2.4$  at  $M = 90$ .<sup>10</sup> However, the use of high Al compositions can result in large bandgap discontinuities with the InGaAs absorption region and in a large breakdown voltage. This work studies the even lower Al composition alloy,  $\text{Al}_{0.55}\text{Ga}_{0.45}\text{AsSb}$ , which can also be

integrated with an InGaAs or GaAsSb absorber for detection out to  $\lambda = 1650$  nm or, due to its smaller bandgap,<sup>11</sup> be utilized as a “reach-through”<sup>12</sup> homojunction structure for NIR detection ( $< \lambda = 1000$  nm). This work presents experimentally determined impact ionization coefficients for  $\text{Al}_{0.55}\text{Ga}_{0.45}\text{AsSb}$  obtained from pure electron and hole-initiated avalanche multiplication ( $M_e$  and  $M_h$ , respectively) measurements, calculated using a local-field model. Measurements of excess noise factor are also presented. The impact ionization coefficients and noise performance of  $\text{Al}_{0.55}\text{Ga}_{0.45}\text{AsSb}$  are then compared with different  $\text{Al}_x\text{Ga}_{1-x}\text{AsSb}$  alloy compositions and a commercially available silicon device.

$\text{Al}_{0.55}\text{Ga}_{0.45}\text{AsSb}$   $p$ - $i$ - $n$  (P1) and  $n$ - $i$ - $p$  (N1) wafers with a nominal  $i$ -region thickness of  $t = 1500$  nm were grown by MBE at a temperature of  $500^\circ\text{C}$  on doped InP (001) substrates as shown schematically in Fig. 1(a). Due to the large miscibility gap of the elements in this material, the  $\text{Al}_{0.55}\text{Ga}_{0.45}\text{AsSb}$  was grown as a short period superlattice with alternating layers of  $t = 0.17$  nm  $\text{Al}_{0.55}\text{Ga}_{0.45}\text{As}$  to  $t = 1.13$  nm  $\text{Al}_{0.55}\text{Ga}_{0.45}\text{Sb}$ , in order to produce the desired alloy and to meet the conditions of lattice matching to InP. Further details of this technique

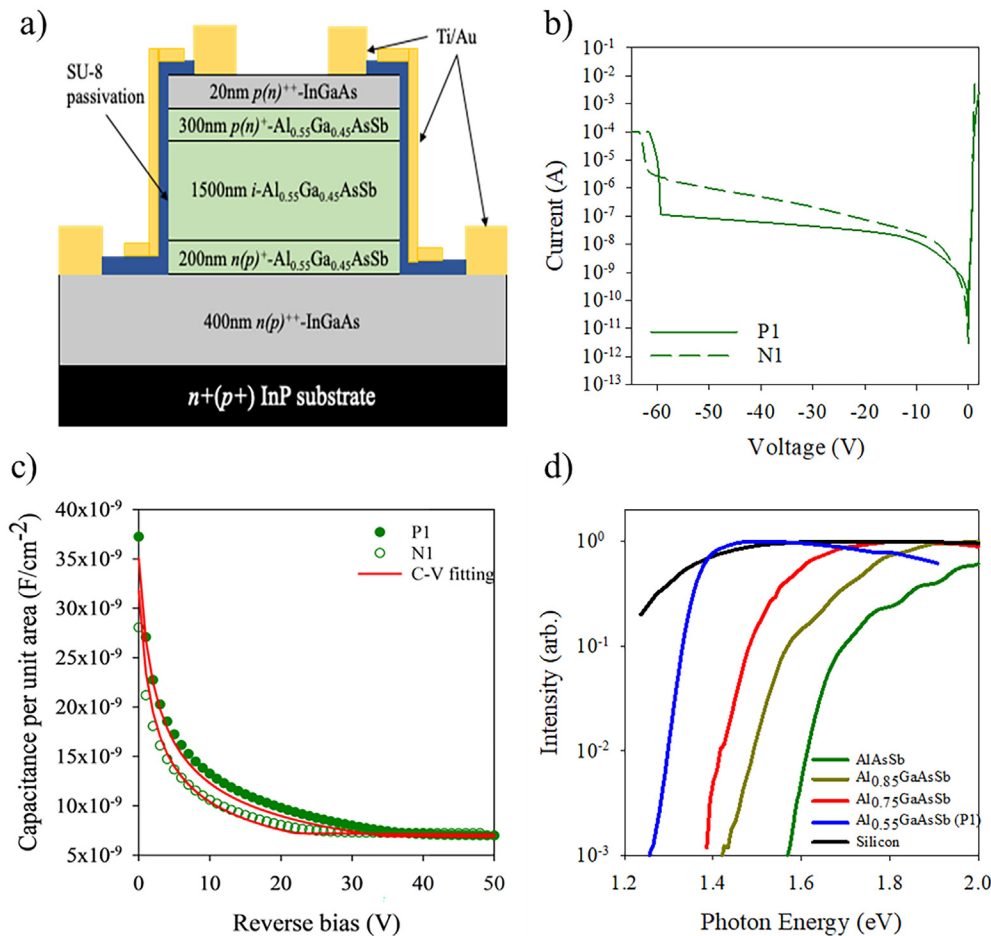


**FIG. 1.** (a) A schematic diagram of the 1500 nm  $p$ - $i$ - $n$  (P1) and  $n$ - $i$ - $p$  (N1) structures. (b) Forward and reverse bias dark current of  $140\ \mu\text{m}$  diameter devices for P1 and N1. (c) Capacitance–voltage data, scaled by area, for P1 and N1. The fitting data used to determine the device region widths and dopings is also shown. (d) Photocurrent spectra for different compositions of AlGaAsSb on InP,<sup>10</sup> compared with a commercial silicon APD (S5973-02).<sup>13</sup>

06 August 2024 08:12:51

can be found in Yi *et al.*<sup>5</sup> The  $p^+$  and  $n^+$  cladding layers of the wafers were nominally  $t = 300$  nm thick with a doping level of  $2 \times 10^{18} \text{ cm}^{-3}$ , and highly doped InGaAs was used for contact layers with a thickness of  $t = 20$  nm for the top and  $t = 400$  nm for the bottom. A wet etching solution of 40 g citric acid: 10 ml  $\text{H}_3\text{PO}_4$ : 10 ml  $\text{H}_2\text{O}_2$ : 240 ml  $\text{H}_2\text{O}$  was used to fabricate mesa diodes of diameters from 70 to 440  $\mu\text{m}$ . Ti/Au contacts were used for both anode and cathode, and the mesa sidewalls were passivated using SU-8 photoresist and an additional layer of Ti/Au in order to prevent optical side injection.

Forward and reverse bias dark currents are depicted in Fig. 1(b). The forward current density indicates negligible series resistance and has an ideality factor of 1.65. The reverse dark currents in both P1 and N1 do not scale with area, suggesting that surface leakage currents may dominate due to 1800 nm mesa depth even at this low Al composition. Figure 1(c) shows that the capacitance-voltage (CV) measurements scale with device area for both P1 and N1. A dielectric constant of 12.4, interpolated from those of AlAsSb<sup>4</sup> and GaAsSb,<sup>14</sup> was used to determine the depletion widths and doping levels by fitting to the CV data. The results indicate that the intrinsic region of P1 has a background doping of  $2 \times 10^{16} \text{ cm}^{-3}$  and is fully depleted at approximately 30 V, while N1 has a background doping of  $1.5 \times 10^{16} \text{ cm}^{-3}$  and is fully depleted at around 25 V. Both structures showed a minimal change in capacitance once the intrinsic regions were fully depleted after  $t = 1500$  nm, indicating high doping ( $>1 \times 10^{18} \text{ cm}^{-3}$ ) in the cladding regions. The depletion width and cladding layer doping levels were further corroborated by secondary ion mass spectroscopy (SIMS) measurements. Despite their similar thicknesses, the small difference in the background doping of the intrinsic regions leads to a difference in the breakdown voltage between P1 (61 V) and N1 (59 V). Figure 1(d) shows the wavelength-dependent spectrum of the  $\text{Al}_{0.55}\text{Ga}_{0.45}\text{AsSb}$   $p$ - $i$ - $n$  (P1), measured using a tungsten halogen bulb and a monochromator at a reverse bias voltage where the intrinsic region was just fully depleted (30 V). The spectrum of  $\text{Al}_{0.55}\text{Ga}_{0.45}\text{AsSb}$  was compared with that of different composition AlGaAsSb alloys. These data confirm the expected decrease in the bandgap with decreasing Al composition, as evident from the change in the absorption cutoff compared to those reported in the literature.<sup>4,7,10</sup> Previous research on high Al composition AlGaAsSb has shown an absorption cutoff limited to  $\lambda = 850$  nm, but the reduction in Al enables detection up to almost  $\lambda = 1000$  nm (1.24 eV). This is approaching a similar cutoff to that of silicon.<sup>15</sup> Figure 2(a) shows photocurrent vs reverse bias for P1 and N1, illuminated using a  $\lambda = 530$  nm laser to ensure “pure” carrier injection conditions, where photogenerated carriers are generated in the top  $p^+$  ( $n^+$ ) cladding layer. The selection of this wavelength was based on previous measurements of  $\text{Al}_{0.75}\text{Ga}_{0.25}\text{AsSb}$ .<sup>10</sup> This means that only electrons (holes) diffuse into the high electric field avalanche region in the  $p$ - $i$ - $n$  and  $n$ - $i$ - $p$  structures, respectively. Measurements were performed using a phase-sensitive technique to remove the contribution of any DC dark currents. There is a large photocurrent increase at low bias (0–10 V) in P1 at  $\lambda = 530$  nm, whereas N1 shows a negligible increase. This indicates that the unintentionally doped region is  $p$ -type, since the photocurrent increases with the depletion edge moving toward the “top” surface with increased reverse bias in P1.<sup>16</sup> The  $p$ - $n$  junction in P1 is at the opposite end of the device to where the carriers are being injected; consequently, the carrier collection efficiency changes significantly as the width of the depletion region

increases. This is because minority electrons generated in the  $p^+$  cladding must diffuse further to be collected by the electric field when the high field region does not extend to the full width of the intrinsic region. This  $p$ -type background doping is also seen in other composition AlGaAsSb alloys and is thought to be due to Ga or Sb vacancies arising in the crystal lattice.<sup>17</sup> The measurement of hole-initiated multiplication requires much higher reverse biases and is limited to  $M_h = 3$  before the onset of edge breakdown. In the  $p$ - $i$ - $n$  structure (P1), challenges arise in accurately determining the multiplication factor as avalanche multiplication may be occurring before the structure is fully depleted. This makes it difficult to discern the true unity gain photocurrent of the device as any increase in photocurrent with bias may be attributed either to avalanche multiplication, or to increased collection efficiency, or to a combination of both. It is therefore necessary to precisely determine the rate of increase due to the changing collection efficiency to accurately calculate the primary photocurrent, and thereby the avalanche multiplication factor. This is particularly critical for the interpretation of excess noise data, as small errors in the calculation of multiplication factor can have a significant effect on the calculated excess noise.<sup>18</sup>

The layer thickness and doping levels for P1 and N1 are known from the C-V and SIMS measurements. With this, the bias-dependent photocurrents seen in P1 and N1 with 530 nm illumination were simulated using a Silvaco TCAD model, with the absorption coefficient, minority carrier diffusion lengths for electrons ( $L_e$ ) and holes ( $L_h$ ), and the ionization coefficients  $\alpha$  and  $\beta$  used as adjustable parameters. The simulated results, shown in Fig. 2(a) as red lines, give excellent agreement with the experimentally measured data (green symbols) with values of the 530 nm absorption coefficient  $\gamma = 2 \times 10^5 \text{ cm}^{-1}$ ,  $L_e = 482$  nm,  $L_h = 100$  nm, and  $\alpha$  and  $\beta$  as given by the Chynoweth expressions in Eqs. (2) and (3).

$$\alpha = \begin{cases} 7.20 \times 10^5 \exp\left(-\left(\frac{1.20 \times 10^6}{E}\right)^{1.4}\right) \text{ cm}^{-1} & \text{when } E < 500 \text{ kV/cm} \\ 6.3 \times 10^5 \exp\left(-\left(\frac{1.20 \times 10^6}{E}\right)^{1.35}\right) \text{ cm}^{-1}, & \text{when } 500 \text{ kV/cm} < E < 564 \text{ kV/cm} \end{cases} \quad (3)$$

$$\beta = \begin{cases} 3.50 \times 10^5 \exp\left(-\left(\frac{1.35 \times 10^6}{E}\right)^{1.46}\right) \text{ cm}^{-1}, & \text{when } E < 500 \text{ kV/cm} \\ 3.50 \times 10^5 \exp\left(-\left(\frac{1.35 \times 10^6}{E}\right)^{1.46}\right) \text{ cm}^{-1}, & \text{when } 500 \text{ kV/cm} < E < 564 \text{ kV/cm} \end{cases} \quad (4)$$

where  $E$  is the electric field.

By deactivating the impact ionization process in the Silvaco TCAD model, the bias-dependent primary photocurrent at a wavelength of 530 nm is obtained, as depicted by the blue lines in Fig. 2(a). The actual multiplication is then determined by calculating the difference between the measured photocurrent and the simulated primary photocurrent and is shown in Fig. 2(b). A numerical random path length model (RPL)<sup>19</sup> was used with the impact ionization coefficients from Eqs. (3) and (4), and electric field distribution profile from C-V measurements to simulate the avalanche multiplication data. This

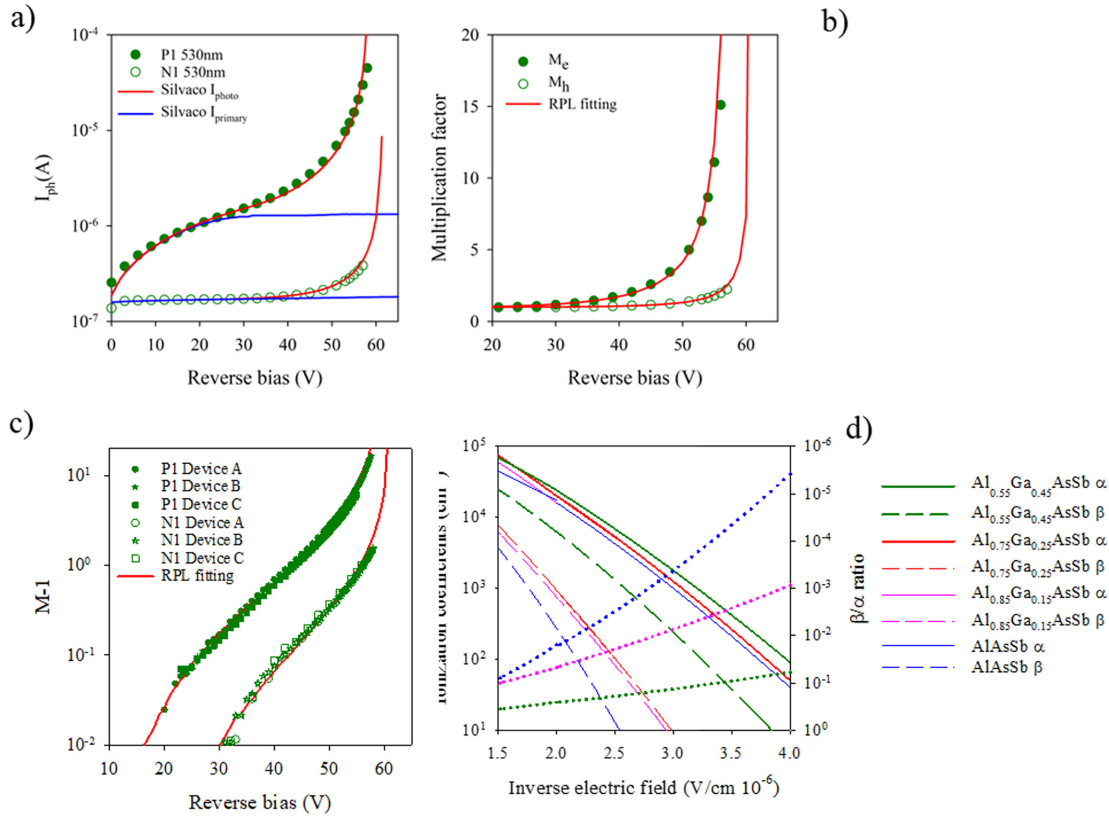


**FIG. 2.** (a) P1 and N1 photocurrent under 530 nm illumination, shown with Silvaco TCAD simulations of primary and multiplied photocurrent. (b) Multiplication factor vs reverse bias voltage for P1 and N1 under 530 nm illumination. (c) Multiplication data for P1 and N1 under pure injection conditions of various devices shown with data simulated by an RPL model, in the form of  $\log(M-1)$ . (d) Impact ionization coefficients for  $\text{Al}_{0.55}\text{Ga}_{0.45}\text{AsSb}$ , compared with other composition of  $\text{AlGaAsSb}$ .<sup>4,6,10</sup> Dotted lines represent  $\beta/\alpha$  ratios for different  $\text{AlGaAsSb}$  compositions as a function of electric field.

model looks at the ionization probability distribution function (PDF) and can include dead-space effects. The agreement was found to be very good, as demonstrated on a log-scale  $M-1$  plot spanning over three orders of magnitude, as seen in Fig. 2(c). The impact ionization coefficients in this model were assumed to be functions only of the local electric field in the structure, meaning that the dead-space effects were not considered. This is a valid assumption in view of the large avalanching widths under investigation. Figure 2(d) illustrates the impact ionization coefficients for  $\text{Al}_{0.55}\text{Ga}_{0.45}\text{AsSb}$  together with other compositions of  $\text{AlGaAsSb}$ . Both  $\alpha$  and  $\beta$  increase (for a given electric field) as the energy bandgap decreases, from  $x=1.0$  to  $x=0.55$ . While both  $\alpha$  and  $\beta$  appear to increase only marginally from  $x=1$  to  $x=0.75$ ,  $\beta$  undergoes a more substantial increase from  $x=0.75$  to  $x=0.55$ . This results in a significantly increased  $\beta/\alpha$  ratio for  $\text{Al}_{0.55}\text{Ga}_{0.45}\text{AsSb}$ , as shown by the dotted lines in Fig. 2(d). Figure 3(a) depicts  $\alpha$  and  $\beta$  for  $\text{Al}_x\text{Ga}_{1-x}\text{AsSb}$  as functions of  $x$  at electric fields of 300 kV/cm and 450 kV/cm. The data suggest that the  $\beta/\alpha$  ratio increases significantly with decreasing Al composition for this alloy system. Conventional McIntyre theory<sup>1</sup> predicts that the excess noise should therefore increase due to the increased  $\beta/\alpha$  ratio.

Excess noise measurements were performed using the TIA based system of Lau *et al.*<sup>18</sup> at a center frequency of 10 MHz and a bandwidth

of 4 MHz. A 530 nm fiber coupled LED was used for illumination. The measured total noise power was calibrated using a silicon photodiode<sup>20</sup> operating with shot noise only, and this was used to calculate the excess noise. The results are shown in Fig. 3(b), with noise data for other  $\text{AlGaAsSb}$  alloys, a 2  $\mu\text{m}$  thick  $\text{InAlAs } p-i-n$  diode<sup>3</sup> and a commercially available silicon APD<sup>21</sup> for comparison. The excess noise for P1 (green symbols) is higher than that seen for  $x=0.75$  but is still relatively low with  $F=2$  when  $M_e=20$ .

Figures 2(d) and 3(a) show that  $\alpha$  only increases marginally as the Al composition decreases from  $\text{AlAsSb}$  to  $\text{Al}_{0.55}\text{Ga}_{0.45}\text{AsSb}$ . By contrast,  $\beta$  appears to increase rapidly over the same composition range, particularly at lower electric fields. Similar but less exaggerated behavior has been observed in  $\text{Al}_x\text{Ga}_{1-x}\text{As}$  and  $(\text{Al}_x\text{Ga}_{1-x})_{0.52}\text{In}_{0.48}\text{P}$ ,<sup>22</sup> with a sudden increase in  $\beta$  when  $x$  becomes smaller than a critical threshold around 0.61. Figure 3(a) shows how the  $\Gamma$  and X-valley energies vary with composition in  $\text{AlGaAsSb}$ .<sup>11</sup> It becomes indirect bandgap semiconductors when the aluminum composition exceeds  $\sim 0.45$ . At aluminum compositions of  $\geq 0.75$ , the  $\Gamma$ -X valley separation is  $> 0.3$  eV so holes in the valence band may not be able to easily ionize with a final electron state in the  $\Gamma$  valley while satisfying the conditions of conservation of energy and momentum, consequently ensuring a low value for  $\beta$ . As the aluminum composition decreases to

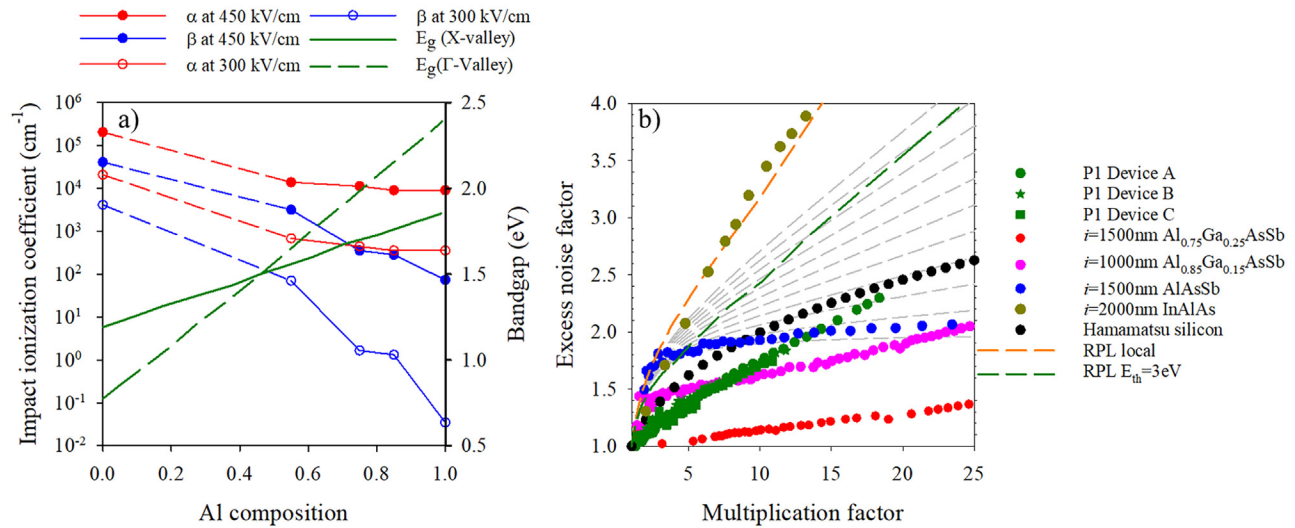


**FIG. 3.** (a) Impact ionization coefficients for different compositions of AlGaAsSb<sup>4,6,10,14</sup> at 300 and 450 kV/cm. Dashed lines show no data point between  $x = 0.55$  and  $x = 0$ . The dashed and solid dark green lines show how the  $\Gamma$  and X valleys vary with Al composition. (b) Excess noise factor for P1 under pure injection conditions (various devices), compared with other compositions of AlGaAsSb with  $x = 1.0$  ( $i = 1500$  nm),<sup>5</sup>  $x = 0.85$  ( $i = 1000$  nm),<sup>7</sup> and  $x = 0.75$  ( $i = 1500$  nm),<sup>10</sup> InAlAs  $p$ - $i$ - $n$  with  $i$ -region thickness of  $2000$  nm<sup>3</sup>, and a commercial Silicon APD, S12023.<sup>21</sup> Orange dashed line is simulated results using an RPL model without dead space effects. Green dashed line shows simulated results using an RPL model incorporating dead space with a threshold energy ( $E_{th} = 3$  eV). Gray dash lines are McIntyre models from  $k = 0$  to  $k = 0.1$  in steps of  $0.01$ .

0.55, the  $\Gamma$  valley energy reduces as does the  $\Gamma$ -X valley separation to 0.1 eV and hole ionization involving the  $\Gamma$  valley may become easier. This mechanism may also explain why  $\beta$  in silicon is so much smaller than  $\alpha$ . The  $\Gamma$ -valley in silicon lies 3.4 eV above the valence band, much higher than the X-valley energy of 1.12 eV.<sup>23</sup> Calculation of the quantum yield for hole ionization in silicon showed that energies of at least 5 eV were needed,<sup>24</sup> much larger than the 4 eV needed for hole ionization in GaAs, which has a larger bandgap of 1.42 eV but with a much smaller energy separation between its  $\Gamma$ -valley and satellite valleys.<sup>23</sup>

The mechanism responsible for the large difference seen in ionization rates for electrons and holes in the AlGaAsSb alloy system at large aluminum compositions was attributed to the fact that most holes gain the threshold energy for ionization from the spin split-off band in materials like GaAs.<sup>24</sup> In GaAs,  $\Delta_{so} = 0.34$  eV, but it is known that this value increases as the atomic number of the group V atom increases. Work done by Liu *et al.*<sup>25</sup> showed that when Bi, with the largest stable group V, was added to GaAs,  $\Delta_{so}$  increased rapidly and this caused a significant reduction in  $\beta$  and consequently reduced the excess noise. GaSb has a larger  $\Delta_{so}$  of  $\sim 0.6$  eV so we estimate that AlGaAsSb will have  $\Delta_{so}$  of  $\sim 470$  meV. This will make it harder for holes to transfer from the heavy hole and light hole bands into the split-off band, and consequently, this reduces  $\beta$  in this alloy system compared to InP or InAlAs. Interestingly, Al<sub>0.55</sub>Ga<sub>0.45</sub>AsSb has an  $\beta/\alpha$  ratio that is not dissimilar to that seen in InAlAs. Although  $F_e$  measured for the Al<sub>0.55</sub>Ga<sub>0.45</sub>AsSb is larger than that in the higher-Al composition alloys studied till date, it is still significantly lower than that predicted by McIntyre's theory and its  $\beta/\alpha$  ratio, shown by the orange dashed line in Fig. 3(b). Even the inclusion of an ionization threshold energy of 3 eV and dead space effects (green dashed line) in the RPL model cannot reduce the excess noise to the levels measured

experimentally. Its excess noise is smaller than that of some commercial silicon APDs and about half that of equivalent InAlAs structures as shown in Fig. 3(b). Ong *et al.*<sup>26</sup> showed that the shape of the ionization probability density function (PDF) in thick AlAsSb was not an exponential but had a non-exponential "peaked" Weibull Fréchet shape. Lewis *et al.*<sup>7</sup> showed from simulations that the multiplication and lower excess noise seen in Al<sub>0.85</sub>Ga<sub>0.15</sub>AsSb can be explained by a Weibull Fréchet PDF. A direct comparison of our results here with the Al<sub>0.85</sub>Ga<sub>0.15</sub>AsSb  $p$ - $i$ - $n$  is complicated by the fact that the latter has only a  $1 \mu\text{m}$  thick avalanching structure and has a lower background doping. The experimental results reported here indicate that a similar effect may be at play even in this lower-aluminum Al<sub>0.55</sub>Ga<sub>0.45</sub>AsSb alloy, and that the presence of the Sb atom results in a more deterministic impact ionization PDF.

D.L.H. acknowledges financial support provided by the S<sub>r</sub> Cymru National Research Network in Advanced Engineering and Materials. S.Y.X. acknowledges financial support from the European Regional Development Fund through the Welsh Government. X.J. and H.I.J.L. contributed equally to data acquisition and data analysis. S.Y.X. and B.L.L. designed the structure and performed material growth and preliminary characterization. S.Y.X. and X.J. are responsible for the device fabrication. X.Y. and C.H.T. supported the results analysis. J.P.R.D. supervised the project. X.J., H.I.J.L., and J.P.R.D. wrote the manuscript. All authors reviewed and approved the manuscript.

## AUTHOR DECLARATIONS

### Conflict of Interest

The authors have no conflicts to disclose.

## Author Contributions

Xiao Jin and Harry I. J. Lewis contributed equally to this work.

**Xiao Jin:** Conceptualization (lead); Data curation (lead); Formal analysis (lead); Writing – original draft (lead); Writing – review & editing (lead). **Harry Lewis:** Conceptualization (lead); Data curation (lead); Formal analysis (lead); Validation (lead). **Xin Yi:** Formal analysis (supporting); Writing – review & editing (supporting). **Shiyu Xie:** Formal analysis (supporting); Writing – review & editing (supporting). **Baolai Liang:** Formal analysis (supporting); Methodology (equal); Writing – review & editing (supporting). **Diana Huffaker:** Formal analysis (supporting); Funding acquisition (equal); Writing – review & editing (supporting). **Chee Hing Tan:** Formal analysis (supporting); Writing – review & editing (equal). **John P. R. David:** Conceptualization (lead); Formal analysis (lead); Funding acquisition (lead); Project administration (lead); Writing – original draft (equal); Writing – review & editing (lead).

## DATA AVAILABILITY

The data that support the findings of this study are available from the corresponding author upon reasonable request.

## REFERENCES

- R. J. McIntyre, “Multiplication noise in uniform avalanche diodes,” *IEEE Trans. Electron Devices* **ED-13**(1), 164–168 (1966).
- L. J. J. Tan, J. S. Ng, C. H. Tan, and J. P. R. David, “Avalanche noise characteristics in submicron InP diodes,” *IEEE J. Quantum Electron.* **44**(4), 378–382 (2008).
- Y. L. Goh, A. R. J. Marshall, D. J. Massey, J. S. Ng, C. H. Tan, M. Hopkinson, J. P. R. David, S. K. Jones, C. C. Button, and S. M. Pinches, “Excess avalanche noise in  $\text{In}_{0.52}\text{Al}_{0.48}\text{As}$ ,” *IEEE J. Quantum Electron.* **43**(6), 503–507 (2007).
- X. Yi, S. Xie, B. Liang, L. W. Lim, X. Zhou, M. C. Debnath, D. Huffaker, C. H. Tan, and J. P. R. David, “Demonstration of large ionization coefficient ratio in  $\text{AlAs}_{0.56}\text{Sb}_{0.44}$  lattice matched to InP,” *Sci. Rep.* **8**(1), 8–13 (2018).
- X. Yi, S. Xie, B. Liang, L. W. Lim, J. S. Cheong, M. C. Debnath, D. L. Huffaker, C. H. Tan, and J. P. R. David, “Extremely low excess noise and high sensitivity  $\text{AlAs}_{0.56}\text{Sb}_{0.44}$  avalanche photodiodes,” *Nat. Photonics* **13**(10), 683–686 (2019).
- B. Guo, X. Jin, S. Lee, S. Z. Ahmed, A. H. Jones, X. Xue, B. Liang, H. I. J. Lewis, S. H. Kodati, D. Chen, T. J. Ronningen, C. H. Grein, A. W. Ghosh, S. Krishna, J. P. R. David, and J. C. Campbell, “Impact ionization coefficients of digital alloy and random alloy  $\text{Al}_{0.85}\text{Ga}_{0.15}\text{As}_{0.56}\text{Sb}_{0.44}$  in a wide electric field range,” *J. Lightwave Technol.* **40**(14), 4758–4764 (2022).
- H. I. J. Lewis, X. Jin, B. Guo, S. Lee, H. Jung, S. H. Kodati, B. Liang, S. Krishna, D. S. Ong, J. C. Campbell, and J. P. R. David, “Anomalous excess noise behavior in thick  $\text{Al}_{0.85}\text{Ga}_{0.15}\text{As}_{0.56}\text{Sb}_{0.44}$  avalanche photodiodes,” *Sci. Rep.* **13**(1), 9936 (2023).
- S. Lee, X. Jin, H. Jung, H. Lewis, Y. Liu, B. Guo, S. H. Kodati, M. Schwartz, C. Grein, T. J. Ronningen, J. P. R. David, J. C. Campbell, and S. Krishna, “High gain, low noise 1550 nm GaAsSb/AlGaAsSb avalanche photodiodes,” *Optica* **10**(2), 147–154 (2023).
- X. Collins, B. White, Y. Cao, T. Osman, J. Taylor-Mew, J. S. Ng, and C. H. Tan, “Low-noise AlGaAsSb avalanche photodiodes for 1550 nm light detection,” *Proc. SPIE* **12417**, 124170K (2022).
- X. Jin, H. I. J. Lewis, X. Yi, S. Xie, B. Liang, Q. Tian, D. L. Huffaker, C. H. Tan, and J. P. R. David, “Very low excess noise  $\text{Al}_{0.75}\text{Ga}_{0.25}\text{As}_{0.56}\text{Sb}_{0.44}$  avalanche photodiode,” *Opt. Express* **31**(20), 33141–33149 (2023).
- S. Adachi, *Properties of Semiconductor Alloys [Electronic Resource]: Group-IV, III-V and II-VI Semiconductors* (Wiley Blackwell, Chichester, West Sussex, 2009).
- Laser Components, *Laser Components Data Sheet (Silicon Avalanche Photodiode SAE-Series)* (Laser Components, 2023).
- Hamamatsu, *Hamamatsu Product Datasheet: Si PIN Photodiodes (S5973-02)* (Hamamatsu, 2019).
- H. Jung, S. Lee, Y. Liu, X. Jin, J. P. R. David, and S. Krishna, “High electric field characteristics of GaAsSb photodiodes on InP substrates,” *Appl. Phys. Lett.* **122**(22), 221102 (2023).
- Hamamatsu, *Hamamatsu Product Data Sheet (Silicon APD S16453 Short Wavelength Type APD)* (Ichino-Cho, 2018).
- M. H. Woods, W. C. Johnson, and M. A. Lampert, “Use of a Schottky barrier to measure impact ionization coefficients in semiconductors,” *Solid-State Electron.* **16**(3), 381–394 (1973).
- A. Y. Polyakov, M. Stam, A. G. Milnes, A. E. Bochkarev, and S. J. Pearton, “Schottky barriers of various metals on  $\text{Al}_{0.5}\text{Ga}_{0.5}\text{As}_{0.05}\text{Sb}_{0.95}$  and the influence of hydrogen and sulfur treatments on their properties,” *J. Appl. Phys.* **71**(9), 4411–4414 (1992).
- K. S. Lau, C. H. Tan, B. K. Ng, K. F. Li, R. C. Tozer, J. P. R. David, and G. J. Rees, “Excess noise measurement in avalanche photodiodes using a transimpedance amplifier front-end,” *Meas. Sci. Technol.* **17**(7), 1941–1946 (2006).
- D. S. Ong, K. F. Li, G. J. Rees, J. P. R. David, and P. N. Robson, “A simple model to determine multiplication and noise in avalanche photodiodes,” *J. Appl. Phys.* **83**(6), 3426–3428 (1998).
- OSRAM data sheet, *High Speed PIN-Photodiode(SFH2701)* (OSRAM Opto Semiconductors GmbH, Regensburg, 2008).
- Ichino-Cho, *Hamamatsu Product Data: Si APD(S12023 Sereis)* (Ichino-Cho, 2022).
- H. I. J. Lewis, L. Qiao, J. S. Cheong, A. N. A. P. Baharuddin, A. B. Krysa, B. K. Ng, J. E. Green, and J. P. R. David, “Impact ionization coefficients in  $(\text{Al}_x\text{Ga}_{1-x})_{0.52}\text{In}_{0.48}\text{P}$  and  $\text{Al}_x\text{Ga}_{1-x}\text{As}$  Lattice-Matched to GaAs,” *IEEE Trans. Electron Devices* **68**(8), 4045–4050 (2021).
- M. L. Cohen and J. R. Chelikowsky, in *Electronic Structure and Optical Properties of Semiconductors* (Springer Berlin Heidelberg, 1989), Vol. 75.
- İ. H. Oğuzman, Y. Wang, J. Kolník, and K. F. Brennan, “Theoretical study of hole initiated impact ionization in bulk silicon and GaAs using a wave-vector-dependent numerical transition rate formulation within an ensemble Monte Carlo calculation,” *J. Appl. Phys.* **77**(1), 225–232 (1995).
- Y. Liu, X. Yi, N. J. Bailey, Z. Zhou, T. B. O. Rockett, L. W. Lim, C. H. Tan, R. D. Richards, and J. P. R. David, “Valence band engineering of GaAsBi for low noise avalanche photodiodes,” *Nat. Commun.* **12**(1), 4784 (2021).
- D. S. Ong, A. H. Tan, K. Y. Choo, K. H. Yeoh, and J. P. R. David, “Weibull-Fréchet random path length model for avalanche gain and noise in photodiodes,” *J. Phys. D* **55**(6), 065105 (2022).